BASIC FEATURES OF THE STS/SPACELAB VIBRATION ENVIRONMENT

C. R. Baugher* and N. Ramachandran+

*NASA Marshall Space Flight Center, Huntsville, Alabama
+Universities Space Research Association, Huntsville, Alabama

ABSTRACT

The Space Shuttle acceleration environment is characterized. The acceleration environment is composed of a residual or quasi-steady component and higher frequency components induced by vehicle structural modes and the operation of onboard machinery. Quasi-steady accelerations are generally due to atmospheric drag, gravity gradient effects, and rotational forces. These accelerations tend to vary with the orbital frequency (~10^{-4} Hz) and have magnitudes ≤ $10^{-6}g_0$ (where 1 g_0 is terrestrial gravity). Higher frequency g-jitter is characterized by oscillatory disturbances in the 1-100 Hz range and transient components. Oscillatory accelerations are related to the response of large flexible structures like antennae, the Spacelab module, and the Orbiter itself and to the operation of rotating machinery. The Orbiter structural modes in the 1-10 Hz range, are excited by oscillatory and transient disturbances and tend to dominate the energy spectrum of the acceleration environment. A comparison of the acceleration measurements from different Space shuttle missions reveals the characteristic signature of the structural modes of the Orbiter overlaid with mission specific hardware induced disturbances and their harmonics. Transient accelerations are usually attributed to crew activity and Orbiter thruster operations. During crew sleep periods, the acceleration levels are typically on the order of $10^{-6}g_0$ (1 micro-g). Crew work and exercise tends to raise the accelerations to the $10^{-3}g_0$(1 milli-g) level. Vernier reaction control system firings tend to cause accelerations of $10^{-4}g_0$, while primary reaction control system and Orbiter maneuvering system firings cause accelerations as large as $10^{-2}g_0$. The use of vibration isolation techniques (both active and passive systems) during crew exercise have shown to significantly reduce the acceleration magnitudes.

INTRODUCTION

The acceleration environment encountered in low Earth orbit is generally composed of three components: quasi-steady, oscillatory, and transient accelerations[1-2]. The low-gravity environment on board the NASA Space Shuttle Orbiters has been measured with a variety of instruments since the

Joint "L+1" Science Review for USML-1 and USMP-1 with the Microgravity Measurement Group, September 22-24, 1993, Huntsville, Alabama, USA.

inception of the Shuttle Program. Understanding the Orbiter acceleration environment is the first step not only in the conception and design of a microgravity experiment, but also in the post flight analysis of the results from the experiment. The under pinning of this acceleration measurement and characterization effort is to provide continuity and a concentrated focus for the analysis, interpretation, and dissemination of these observation on space missions. This approach allows the results of a variety of measurements to be organized into a technical investigation which evolves from discovery, to analysis, to synthesis. An overview of the shuttle acceleration environment is provided in this paper. The reader is referred to [3-6 and the references cited therein] for detailed information about specific issues. In section 2, the shuttle coordinate system and mission flight attitudes are introduced. In section 3 we describe the different acceleration classifications and summarize acceleration measurements made to date. In this section, we also focus on crew exercise activity as measured and recorded by the NASA Space Acceleration Measurement System (SAMS). The use of vibration isolation systems in reducing the impact to the acceleration environment is also discussed.

I. SPACE SHUTTLE COORDINATE AXIS AND FLIGHT ATTITUDES

The Orbiter coordinate axes and flight attitudes or orientations are first explained. The Orbiter Structural coordinate system shown in Fig. 1, is Orbiter-fixed with the origin in the Orbiter plane of symmetry, 400 inches below the center line of the Orbiter cargo bay. The most forward Y-Z plane of the cargo bay is at X = 582 inches. The X_0 axis is in the Orbiter plane of symmetry, parallel to and 400 inches below the centerline of the cargo bay. Positive sense is from the nose toward the tail. The Z_0 axis is in the Orbiter plane of symmetry and perpendicular to the X_0 axis The positive sense for this axis is upward in the landing attitude as shown in the figure. The Y_0 axis completes the right hand, orthogonal coordinate system.

A schematic representation of the two most frequently used attitudes or orientations for flying microgravity missions is shown in Fig. 2. In the *Z-local vertical* attitude, the vehicle's z-axis (out of the cargo bay) is oriented along the radius vector to the center of the Earth. This attitude has somewhat lower drag, but requires more thruster firings to maintain the attitude. The second is the *gravity-gradient* attitude. In this case, the vehicle's center line (x axis) is along the radius vector. This attitude is inherently stable and minimizes the thruster firings at the expense of more drag[3]. During the flight of the first US Microgravity Laboratory (USML-1) in June 1992, the shuttle was flown in the *gravity-gradient* attitude during the use of the Crystal Growth Furnace (CGF) for the growth of several semiconductor crystals.

II. ORBITER ACCELERATION ENVIRONMENT

The accelerations experienced in a manned orbiting space laboratory are loosely classified as quasi-steady, oscillatory, and transient. The quasi-steady classification, by convention, is assigned to accelerations with frequency below about 0.01 Hz. This encompasses accelerations due to atmospheric drag, gravity gradient effects, and rotational forces. Using atmospheric models, the contribution from atmospheric drag on the Shuttle Orbiter is estimated to be on the order of $10^{-6}g_0$ [2]. This contribution varies with the orbital frequency of about 10^{-4} Hz.

Gravity gradient accelerations are related to the physical displacement of an experiment from the center of mass of the orbiting laboratory. The effect arises from the force imparted by the structure of the vehicle on the experiment, as the vehicle drags the experiment in the vehicle's orbit. Without the structure, the experiment would diverge into a slightly different orbit because of its displacement from the Orbiter center of mass. The magnitude of the force is dependent on the amount of displacement between the experiment and the vehicle's center of mass; the magnitude also differs depending on whether displacement is in the orbit plane, or perpendicular to it[3]. In general, the gravity gradient effect is on the order of $10^{-7}g_0$ per meter from the Orbiter center of mass. Rotational effects are on the order of 10^{-8} g_0. Overall, depending on location, atmospheric drag or gravity gradient effects dominate the quasi-steady regime on the Shuttle Orbiter contributing to a total magnitude on the order of $10^{-6}g_0$ with frequency about 10^{-4} Hz .

Higher frequency accelerations experienced in low Earth orbit are generally referred to as g-jitter. In the 1 to 100 Hz range, measured accelerations on the Shuttle are usually related to the excitation of structural modes by oscillatory and transient sources. Vehicle maintenance and communications, experiment pumps, fans, and motors are all common oscillatory sources on an Earth orbiting laboratory. Common transient sources are nominal crew activity and exercise, and Orbiter thruster firings for attitude control and maneuvering. Acceleration levels on the Shuttle Orbiters related to such sources vary from 10^{-4} g_0 (oscillatory, light crew activity, Vernier Reaction Control System (VRCS) firings) to 10^{-2} g_0 (Primary Reaction Control System (PRCS) firings and Orbiter Maneuvering System (OMS) burns). Reports of acceleration measurements from various systems are available in the literature [see for instance, the references cited in 7].

A. Quasi-steady measurements - Orbital Acceleration Research Experiment (OARE)

The OARE is a state-of-the-art accelerometer system which is used for obtaining highly sensitive, low frequency measurements of the flight acceleration environment in combination with in situ calibration. The measurement system includes a very sensitive three-axis accelerometer, a full in-flight

calibration station, and a control microprocessor which can provide custom in-flight data processing and storage. The measurement system is built around a Bell Textron Miniature Electro-Static Accelerometer (MESA). The associated calibration station is a two-axis rate table which allows the instrument to be rotated at fixed rates to verify instrument performance parameters. The rotation serves the dual function of imposing a known centripetal acceleration on the accelerometer and allowing the individual axes to be inverted to separate fixed instrument biases from actual acceleration effects of the ambient environment. The OARE is designed for characterizing the Orbiter's aerodynamic acceleration along its principal axes at orbital altitudes and in the transition regime during re-entry. Therefore, the instrument has been optimized for measurements in a very low frequency regime and for amplitudes of a micro-g and less. The NASA Microgravity Science and Applications Division (MSAD) sponsors the OARE flights, which to date has flown on four missions in the Shuttle cargo bay. Table 1 identifies the OARE missions flown to date.

OARE flew on its second flight on STS-50 (USML-1), which was a mission dedicated to science, particularly to the study of the effects of reduced gravity on a variety of fundamental physical processes. The basic Shuttle/Spacelab flight configuration for the flight was the long Spacelab module with mission related experiments in both the Spacelab and the middeck area. A major goal of the mission's scientific investigations was the study of the sensitivity of the growth of semiconductor crystals to the effects of low-level, quasi-steady residuals. Pre-flight mathematical modeling of experiments in the Crystal Growth Furnace (CGF) facility indicated possible adverse responses of the experiments to long-period accelerations as low as a few tenths of a micro-g, if those forces were perpendicular to the longitudinal axis of the crystal. To avoid such forces during the experiment intervals, the CGF was located within two meters of the vehicle center of mass to minimize gravity gradient forces, and the vehicle was flown in a special attitude during experiment runs to direct drag forces parallel to the crystal axis.

The most important finding by the OARE instrument during the flight was the apparent presence of an anomalous force along the vehicle x-axis. A short section of the analyzed data from Ref. 8 is shown in Fig. 3. The gravity gradient mode for the flight had been carefully engineered to minimize the forces in this direction and pre-flight predictions had been for this component to average near zero. This section of data indicates a residual force of the order of 0.5 micro-g's was present for extended portions of the mission. The conclusion from analysis was that the Orbiter was creating the observed environment. The acceleration in the y-axis is slightly negative ($\approx$ 0.2 micro-g) mostly due to aerodynamics and out-of-plane effects. The z-axis acceleration shows the day/night atmospheric effect, about 0.6 micro-gs. The OARE measurements on USML-1 clearly demonstrated the need for in-flight measurements due to two reasons: 1) to monitor and record the residual g level for subsequent

comparison to predicted theoretical models and 2) to correlate departures (in the residual g level) from predictions and experiment requirements, to observed experiment results.

B. Oscillatory and transient disturbance measurements - Space Acceleration Measurement System (SAMS)

SAMS was developed at the NASA Lewis Research Center for MSAD to serve as a standard accelerometer system for all MSAD-sponsored Orbiter microgravity missions. SAMS consists of three remote triaxial sensor heads, connecting cables, and a controlling data acquisition unit with a digital data recording system using optical disks with 200 megabyte storage capacity per side. With the availability of crew access to change the disks, data storage capacity is essentially unlimited. SAMS can be configured to fly in the Orbiter mid-deck, in the Spacelab module, and in the Orbiter cargo bay. To date, SAMS has flown on ten missions and has flown in all three configurations. We present here some results from the first Spacelab Life Sciences mission (SLS-1) which flew on Columbia in June 1991 on STS-40, USML-1 which flew on Columbia in June 1992 on STS-50, and the first United States Microgravity Payload (USMP-1) which flew on Columbia in October 1992 on STS-52. SAMS missions to date are identified in table 2. The individual SAMS heads are usually configured for different frequency ranges and located at areas of specific interest. For example, on STS-50, SAMS heads were located at 3 different locations in the Spacelab module; on rack 10 of Spacelab on the bottom of the Glovebox facility with a low pass cut-off frequency of 25 Hz, on rack 5 on the Surface Tension Driven Convection Experiment with a 5 Hz cut-off frequency, and on rack 9 on the Crystal Growth Furnace with a cut-off frequency of 2.5 Hz to monitor low frequency accelerations. Data sampling is typically done at five times the cut-off frequency. Data from these and other missions and from other accelerometer systems suggest that the low-gravity environment is fairly consistent between missions even with different payloads, configurations, and Orbiters[4].

The SAMS data analysis comprises of 3 distinct steps: 1) Initial data recording and processing. This step involves in-flight data recording along with measurements of sensor temperature, gain setting, ancillary engineering data and a time record, 2) Post flight processing that involves corrections if any for temperature sensitivity, physical misalignments, electronic bias and filtering, etc., and 3) Final data presentation and analysis using time and frequency domain plots. Steps 2 and 3 mentioned above are usually carried out together as a combined analysis procedure. Error analysis indicates that SAMS measurements are typically accurate to the order of 10% when the data is completely within the dynamic range for the selected gain of each accelerometer. Measurement errors stem from both the accelerometer and the data system and is the result of numerous factors, including calibration error, random drift, noise and rectification error.

The algorithms and data presentations designed for the analysis mentioned in step 3 above, were formulated to summarize a very large volume of data on long term (2 hour) plots to discriminate periods of significant and reduced activity. To this end, the data is presented across the mission period in a time domain analysis, and expanded in depth by frequency domain analysis over selected intervals. The time domain analysis consists of parallel plots of the acceleration mean and the Root Mean Square (RMS), these forms being analogous to the dc and rms signals used in electrical measurements. The approach was established to separate an approximate indication of the low frequency environment (estimated by the mean) and contrast it with the time varying portion (estimated by the RMS).

The acceleration mean is calculated as the vector magnitude of the arithmetic mean of the acceleration on each axis typically over a 10 second period. To eliminate inaccurate data points attributed to gain change stability transients, transient points are discarded following each gain change[9] and compensated for in subsequent calculations. Estimated instrument bias based on on-orbit values is removed and temperature compensation of bias, is performed before the acceleration mean is calculated. The RMS is similarly calculated as a vector of all 3 axes for each triaxial-sensor head. The mean is very useful to flag a condition in which the accelerometer senses a net acceleration component that is persistent for intervals of the order of ten seconds or more. Therefore, events such as thruster firings that provide a net thrust to the vehicle will be evident, while events internal to the vehicle (such as crew induced impacts) will tend to average out to zero. Fig. 4 shows an example of this processing for a complicated event from STS-40.

In the frequency domain, SAMS data is reported in two formats: 1) as magnitude spectrum color contour charts and 2) as Power Spectral Density (PSD) charts. The accelerometer data is first processed by a Fast Fourier Transform (FFT) algorithm. Each FFT is converted to a magnitude spectrum by calculating the vector sum of the real and imaginary parts of the transform at each point and represented as color charts with colors corresponding to the acceleration magnitude. The PSD representation is used to represent the average power, as opposed to the peak acceleration represented by the magnitude spectrum. During the FFT processing, no special windowing functions are implemented to suppress side lobes created by a finite sample interval. The bandwidth associated with the spectrums is noted on each chart to provide a record of the sample size used in the processing. More detail on the data acquisition and reduction procedures can be obtained from the mission summary reports.

Typical low frequency Orbiter structural modes are shown in Fig. 5 from data taken on STS-47. This plot represents the environment during nominal crew activity and is characterized by distinct frequency peaks in the 1-10 Hz range. The term nominal crew activity is used to indicate a time period when no significant acceleration sources such as vehicle maneuvers, water dumps, satellite launches and crew exercise were present. The measured acceleration magnitudes are generally found to vary with

the level of crew activity. Fig. 6 shows an example of the difference in levels during periods of crew sleep, nominal crew activity, and crew exercise on a bicycle ergometer taken on the STS-40 mission[10].

The data in each plot is a PSD calculation performed on 50 seconds of raw SAMS data and presented in units of Micro-g/$Hz^{1/2}$. The RMS value for the data on each chart is shown in the upper right. Acceleration levels in time vary from 10^{-4} to $10^{-3}g_o$. The SAMS sensor, located in rack 5 in the Spacelab module, recorded data at 25 samples/sec with a 5 Hz low pass filter. An important characteristic of the g-jitter environment is that the oscillatory and transient sources tend to excite Orbiter and payload structural modes. Because of this, the effects of a high magnitude transient source may be felt by an experiment in the form of damped ringing for some time after the initial event occurred. The 3.5, 4.7 and 5.5 Hz components are all related to the excitation of structural modes by exercise activity and occasional thruster firings. Note the change of scales in the graphs.

Even during the sleep period, the observation is dominated by the vehicle structural modes, but the general level has decreased by an order of magnitude. An example of the excitation of structural modes by an oscillatory source is the 17 Hz signal (not shown in Fig. 5). The KU-band communications antennae on the Orbiters dithers at ~17 Hz to prevent stiction of the gimbal. This dither frequency tends to excite a 17 Hz Orbiter mode. During USMP-1, the SAMS recorded not only the 17 Hz signal, but also first through fourth harmonics at 34, 51, 68, and 85 Hz. The most interesting feature of this signal is the extreme variability of its signature. Acceleration levels while the antenna was operating varied by an order of magnitude. The source of the variability is presently unknown, but it seems likely that it is related to the pointing angles of the system. Further studies are in progress to evaluate the variability.

C. Shuttle Mechanical Disturbances

Several mechanical systems on the Orbiter induce transient or oscillatory disturbances. The most familiar to investigators is the previously mentioned Ku Band antenna which is used for communications between the vehicle and the Tracking Data Relay Satellite. Other sources of unwanted noise are compressor motors associated with refrigerators, and fans in payloads. The most complex disturbance originates from remote manipulator system (RMS). This system is the jointed arm located in the Shuttle's cargo bay and used for grappling satellites or other pieces of space hardware which need to be manipulated by the crew from within the flight deck.

Disturbances in the raw accelerometer data, such as the one shown in the upper right box in Fig. 7, are readily visible when the RMS is operated. Although the disturbances were generally expected, their analysis reveled some unusual properties. The main section of the plot of Fig. 7 shows these characteristics over a fifteen minute stretch of data while the unit was being operated. The upper trace in this plot is the one second averages of the raw accelerometer data from the vehicle's z-axis. The most

unusual feature is the steady offset lasting for about a minute in the 50 to 100 micro-g range starting about 9 minutes into the plot. The second trace in the figure is the telemetered data on the motion of the RMS elbow joint. As can be seen, the steady offset correlates (almost) with a robust movement of this joint. On the other hand, it is difficult to understand why movements of the arm would instigate this type of acceleration. The indicated acceleration is sufficient to impart a net change of several centimeters per second in the velocity of this relatively heavy vehicle (about 100000 kg), in a situation in which there is nothing for the arm to push against.

The answer to the puzzle becomes evident when the record of the vehicle attitude control thrusters is examined. The bottom trace in the figure plots a small triangle each time the thrusters fired during the data interval. It is evident that the operation of these thrusters correlates exactly with the interval of the steady offset acceleration. The explanation then, is that the movement of the arm is sufficient to "rock" the vehicle beyond its in-flight stability control limit, generally of the order of 0.1 degree in pitch, yaw, and roll. When this occurs, the thrusters begin operating to steady the attitude. The thrusters do not form a perfect couple and always provide a residual thrust along the z-axis. Clearly, one means of reducing this type of motion would be to open the control limits to minimize the operation of the attitude control system during arm maneuvers.

A second unusual feature of the averaged acceleration data is the large ringing seen in the plot seen at about eight minutes, and again at about nine minutes into the data interval. Although it is not shown here, the initiation of this ringing correlated exactly with short, rapid movements of the RMS shoulder joint. This ringing has been traced to a natural oscillation of the arm in response to short dynamic impulses. Thruster firings alone can induce the response, however at the relatively low amplitude of a few micro-g's.

D. Exercise vibration and isolation

Specific crew exercise related measurements were carried out during STS-50. During the mission, two approaches for minimizing the effects of crew exercise on the acceleration environment in the vehicle were undertaken. One was a special exercise device called EVIS (Ergometer Vibration Isolation System) located in the Orbiter middeck and the other was the suspension of the exercise ergometer from elastic bungee cords on the flight deck. The reader is referred to reference 9 for more detail on these devices. The EVIS system is an upright bicycle ergometer that incorporates three-axis vibration isolation. The second system resembled a recumbent bicycle suspended by a system of elastic bungees (in the X and Y directions) that also affords some form of vibration isolation. The exercise sequence required a warm-up interval and an interval of high exertion for a total time of 20 to 40

minutes. During the exercise, crew members attempted to maintain a constant pedaling rate of about 70 rpm, or approximately 1.2 Hz.

Some measurements on the ergometer were also made during the STS-40 mission in the Spacelab module. Qualitative analysis of the exercise period acceleration data shows that the fundamental pedaling frequency is observed in the accelerometer measurements. Interestingly, the fundamental is not the most intense signature of the exercise; see Fig. 6, panel 3. The 1.2 Hz frequency is just visible on the compressed scale in the x-axis. The first harmonic at 2.45 Hz is at a somewhat higher magnitude and the largest signature is at the vehicle structural resonance mode of 3.6 Hz.

For the STS-50 mission, the accelerometers were placed at three specific locations in the Spacelab module while crew exercise was carried out on the flight deck and middeck. A cursory look at the data (not shown) during bungee cord isolated exercise routines show that the character of the exercise signature is significantly different. With the bungee isolation, the vehicle modes are no longer excited above their steady state level, but the level of the fundamental exercise frequency is enhanced. For a more rigorous quantitative comparison of the data, four sections of accelerometer data (frequency range dc-5 Hz) corresponding to 1) no exercise or post exercise, 2) EVIS exercise, 3) bungee exercise, and 4) hard mounted exercise, were selected and a separate analysis performed. These plots each represent 10 minutes of activity to average down transient effects and changes in the exercise rate by the same individual. The power spectral density (PSD) from each of the four sections of data is shown in Fig. 8 on a log scale. The PSD is calculated such that

$$RMS = \left[\int_0^f (PSD) df \right]^{1/2} \qquad (1)$$

This implies that the RMS of the time domain signal is equal to the square root of the integral of the PSD of that signal. For this analysis, the upper limit on the integral was be set to 6 Hz. The accelerometer's 5 Hz filter is affecting the data at about the 10% level beyond the 3 Hz point[9].

The fundamental frequency of the exercise is visible in all exercise cases near 1.2 Hz. As one progresses from the case of no exercise through the hard-mounted case, the energy in the vehicle structural modes is seen to steadily increase. There appears to be no large effect by the exercise on the environment below 1 Hz. Additional insight into the data can be gleaned by evaluating the RMS in equation (1) as a function of the upper limit on the integral. This plot labeled *Cumulative RMS* is shown in Fig. 9. At 6 Hz, the value of the integral is equal to the RMS of the original time domain signal. At lower frequencies, the value of the cumulative RMS calculation represents the RMS which would be obtained if there were a sharp low-pass filter in effect at the frequency. The result is one measure of the

effectiveness of the various exercise systems on STS-50. Table 3 summarizes the numerical values at end points corresponding to 2 Hz and 6 Hz, respectively, of this plot.

Based on the data, the distinct reduction in disturbance levels due to vibration isolation is clear. Based on the particular set of exercise sessions used for the plot, the bungee system reduced the integrated disturbance level between 0 and 6 Hz to about one-third of the non-isolated case, while the EVIS reduced the level by about one fourth. From an alternative viewpoint, EVIS allowed the disturbance background to rise by about a factor of two over the no-exercise case (post-exercise on the plot), while the bungee system allowed an approximate 50% additional increase over the EVIS. Considering the relative complexity, expense, and operational difficulties of the EVIS, the present analysis suggests that a bungee system is adequate.

CONCLUSIONS

An overview of the Space Shuttle acceleration environment is provided. Measurements from OARE are used to characterize the residual or quasi-steady environment and measurements from SAMS are used for evaluating the acceleration components at higher frequencies.

The measurement of the quasi-steady environment (frequencies below 0.01 Hz.) by the OARE instrument determined that this portion of the environment can be influenced at a fraction of the micro-g level by forces other than drag and gravity gradients. On STS-50, a persistent acceleration of approximately 0.5 micro-g, thought to be Orbiter induced, was present for much of the mission. Therefore, earlier speculation that this portion of the spectral range could be handled by analytic modeling have been proven incorrect. It is now known that experiments sensitive to forces of this nature will have to depend on a measurement system with the demonstrated capabilities of the OARE (of the order of 0.1 micro-g absolute) to supply environmental data for post-flight analysis.

In the lower frequencies (1 to 10 Hz), it has been determined that the dominant pattern of the STS environment is the presence of enhanced disturbances levels at a set of vehicle resonance modes which form a fairly common background from mission to mission. Above this frequency range (10 to 100 Hz), disturbances to the environment are primarily generated by noisy equipment. A notable exception is the 17 Hz dither of the STS Ku-band TDRSS communication antenna. On occasion, this disturbance has been found to account for a major portion of the total noise power in the 0-100 Hz frequency range.

The disturbance contributions originating from crew activity arise mostly in the 1 to 10 Hz frequency band. They range from a gentle rocking of the vehicle during intervals when the crew is performing routine duties, to fairly violent shaking and excitation of the structural modes during robust exercise periods. Tests show however, that the exercise disturbances can be substantially reduced by combining the exercise equipment with vibration isolation techniques.

REFERENCES

1. Ostrach, S., 1982, "Low Gravity Fluid Flows, Annual Review of Fluid Mechanics, Vol. 14, pp. 313-345.

2. Hamacher, H. and U. Merbold., "Microgravity environment of the Material Science Double Rack on Spacelab-1," J. Spacecraft, Vol. 24, No. 3, pp. 264-269, 1987.

3. Baugher, C. R., *Acceleration Characterization and Analysis Project (ACAP)* - 1992 Annual Report, NASA Marshall Space Flight Center, 1993.

4. Baugher, C. R., Martin, G. L., and DeLombard, R., "Review of the Shuttle Vibration Environment," AIAA Aerospace Sciences Meeting, Reno, Nevada, AIAA 93-0832.

5. Rogers, M. J. B., Alexander, J. I. D., 1992, "Residual Acceleration Data Analysis for Spacelab Missions," Microgravity Sci. Tech. V, pp. 43-49, 1993.

6. Blanchard, R. C., Nicholson, J. Y., Ritter, J. R., "STS-40 Orbital Acceleration Research Experiment Flight Results During a Typical Sleep Period," NASA Technical Memorandum 104209,1992.

7. Ramachandran, N, Baugher, R. C., and Rogers, M, J, B., "Acceleration Environment of the Space Shuttle and its Impact on Thermo-Solutal Fluid Mechanics," ASME Winter Annual Meeting, New Orleans, Nov. 28 - Dec. 3, AMD-Vol. 174, FED Vol. 175, pp. 155-171, 1993.

8. Blanchard, R. C., Nicholson, J. Y., and Ritter, J. R., "Preliminary OARE Absolute Acceleration Measurements on STS-50," NASA TM 107724, Feb. 1993.

9. Baugher, C. R., *Early Summary Report of Mission Acceleration Measurements from STS-50,* 1992.

10. Baugher, C. R., *Early Summary Report of Mission Acceleration Measurements from STS-40,*1991.

Table 1: OARE Missions

Mission Id.	Launch Date	Mission
STS-40	June 5, 1991	First Life Science Laboratory
STS-50	June 25, 1992	First US Microgravity Laboratory
STS-58	Oct. 18, 1993	Second Life Science Laboratory
STS-62	March 4, 1994	Second US Microgravity Payload

Table 2: Specific Space Shuttle missions and SAMS Configuration

Mission Id.	Launch Date	Mission
STS-40	June 5, 1991	First Life Science Laboratory
STS-42	Jan. 22, 1992	First International Laboratory
STS-43	Aug. 2, 1991	TDRSS Launch
STS-47	Sept. 12, 1992	Spacelab - Japan
STS-50	June 25, 1992	First US Microgravity Laboratory
STS-52	Oct. 22, 1992	First US Microgravity Payload
STS-54	Jan. 13, 1993	TDRSS Launch
STS-57	June 23, 1993	First Spacehab Mission
STS-60	Feb. 3, 1994	Second Spacehab Mission
STS-62	March 4, 1994	Second US Microgravity Payload

Table 3: Cumulative RMS Values

Exercise Mode	RMS 0-2 Hz (micro-g)	RMS 0-6 Hz (micro-g)
Hard Mounted	42.2	456
Bungee	38.6	159
EVIS	26.3	110
No Exercise	22.1	73

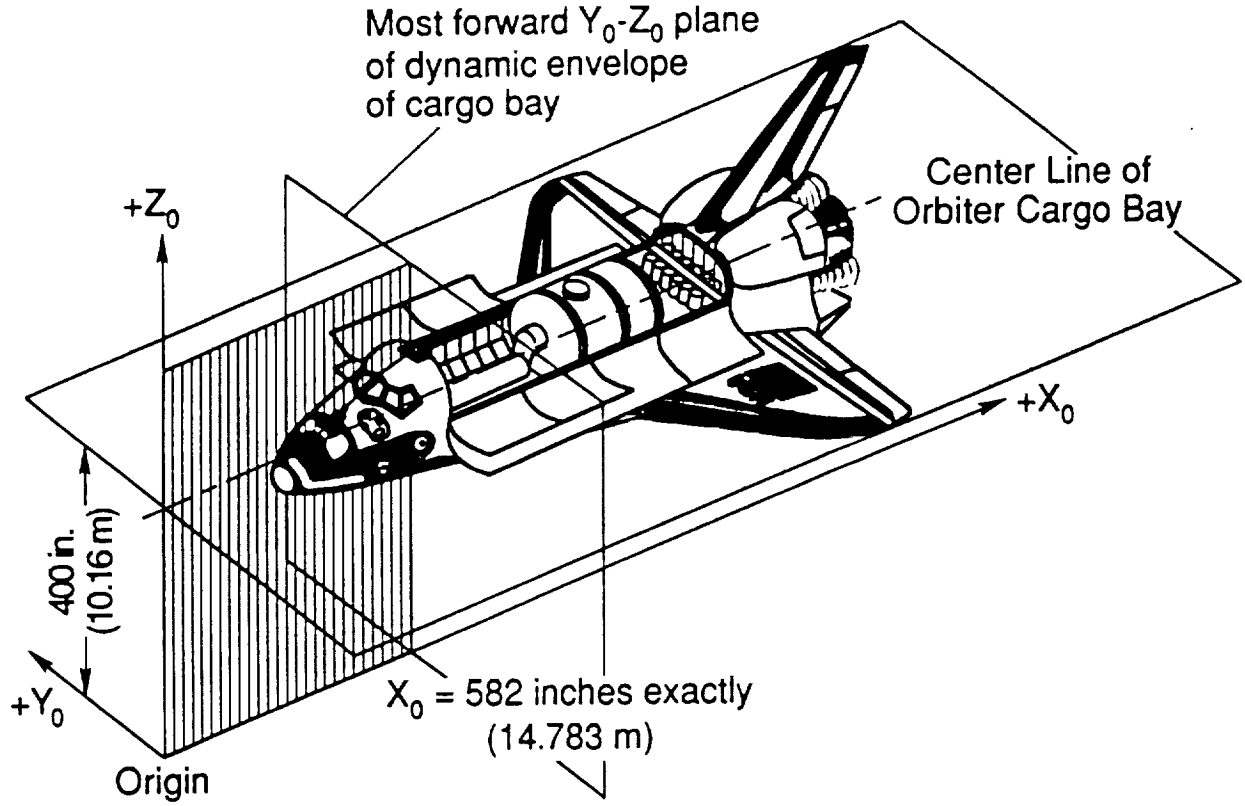

Figure 1 The Orbiter Structural Coordinate System (X_0, Y_0, Z_0).

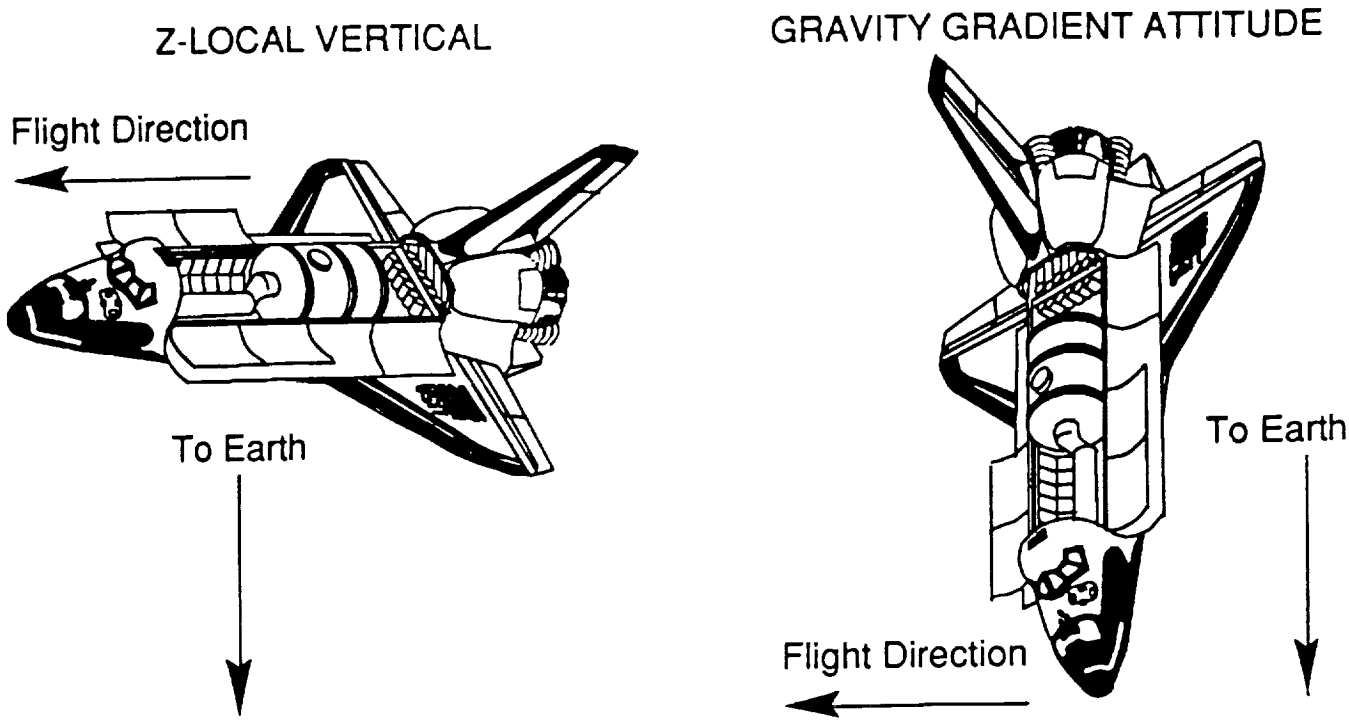

Figure 2 Space Shuttle flight attitudes.

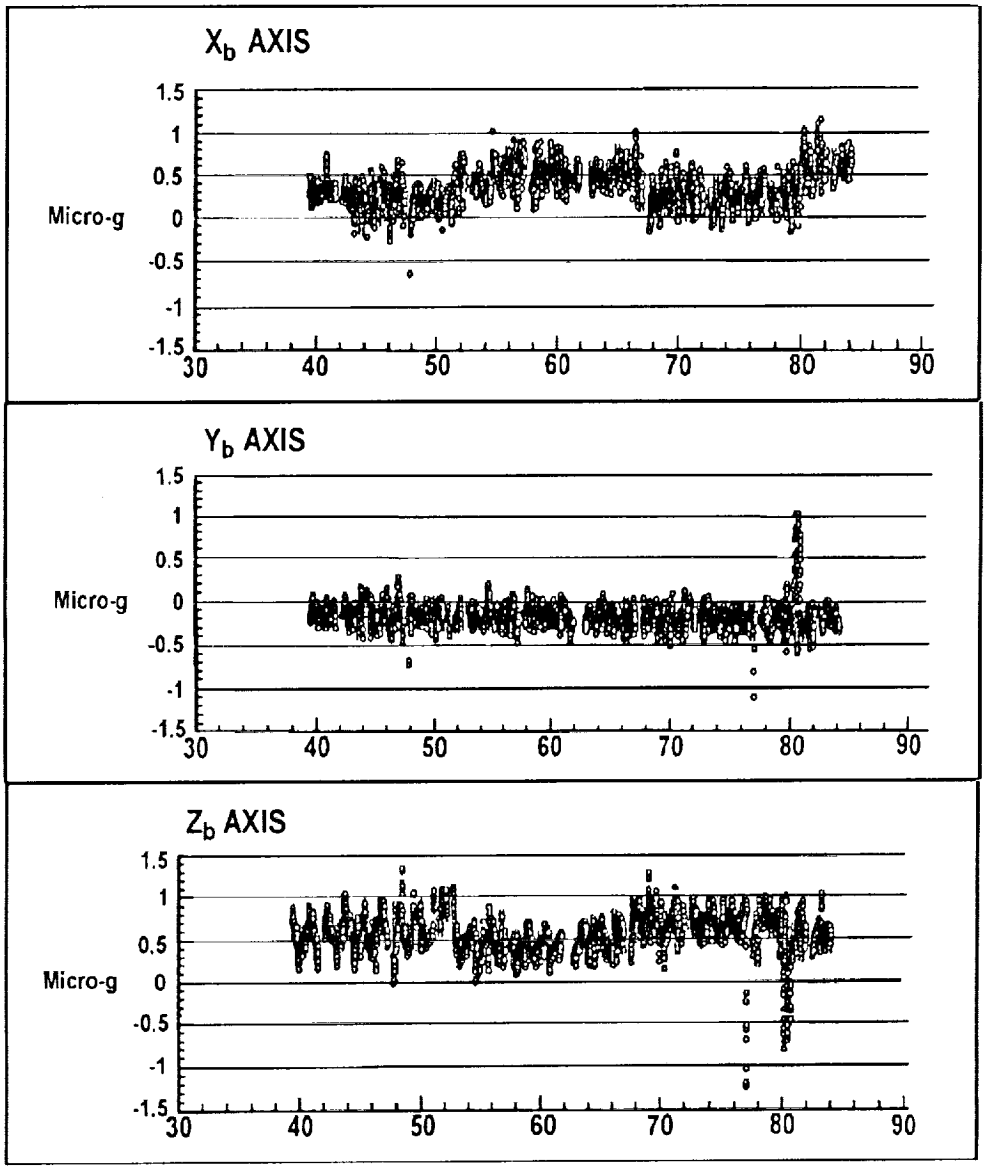

Figure 3 Quasi-steady measurements from OARE on USML-1 (Ref. 8).

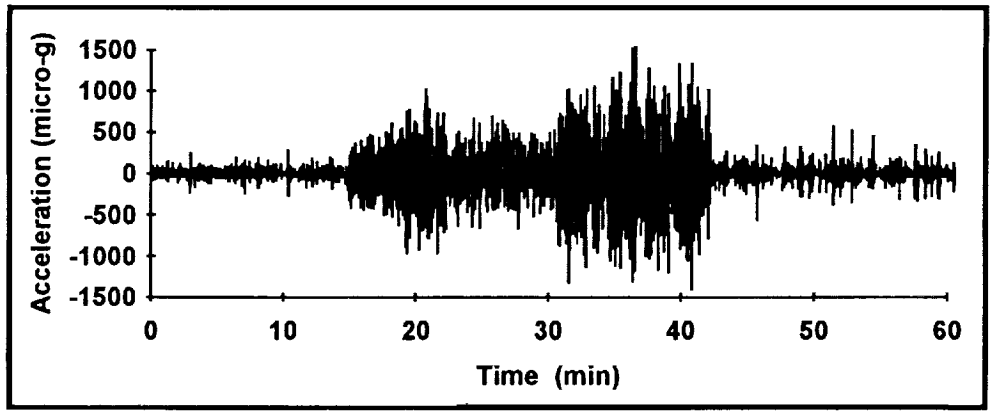

a) Raw Data from z-axis accelerometer

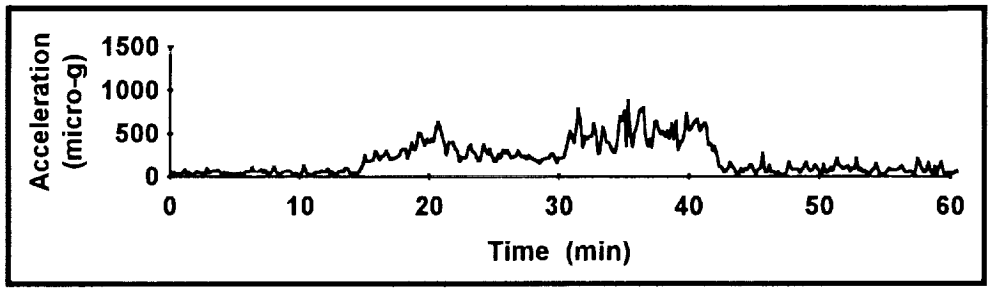

b) RMS values calculated from each 10-second interval

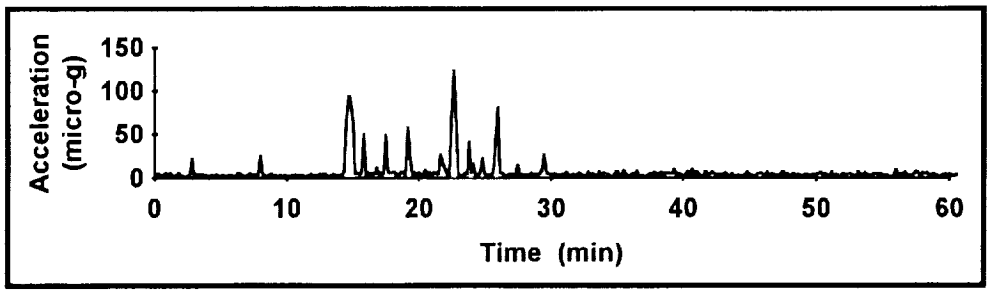

c) Acceleration means calculated from each 10-second interval

Figure 4 Summary Processing of Raw Acceleration Measurements

The initial analysis of SAMS data was designed to reduce the large volume of data, yet preserve its salient features. The raw data in 4a) contains approximately 90,000 measurements over the one-hour interval. The two sets of processed data contain 360 data points each. This data was selected from a period in which there were two dissimilar events in progress. The predominate was an approximate thirty-minute crew exercise session evident in the center portion of the raw data and the RMS processing. Coincident with the beginning of the exercise, a vehicle attitude maneuver was implemented which involved thruster firings. The residuals from these firings are clearly evident in the acceleration means in 4c). Note the expansion of the scale by a factor of ten in 4c) and the "disappearance" of the large perturbations due to the crew activity since it does not impart net forces on the 10-second averaging basis.

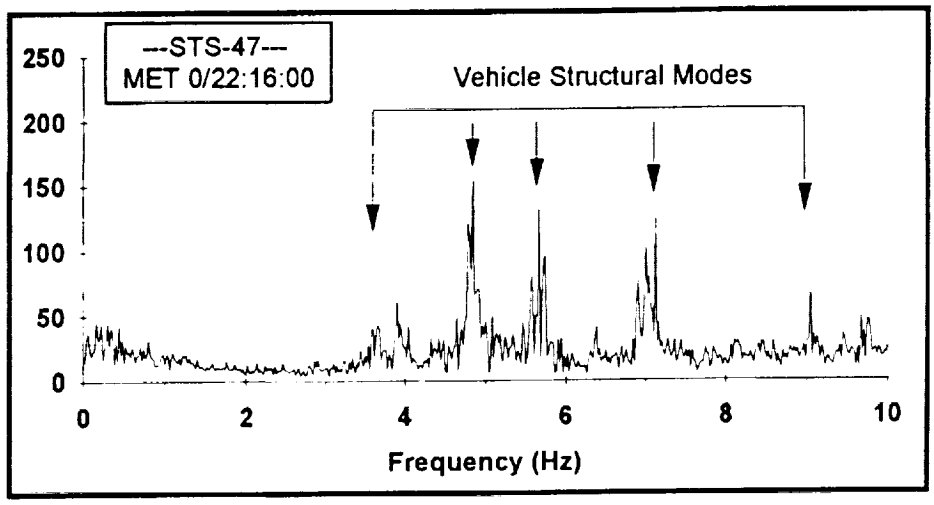

Figure 5 Typical low frequency STS structural modes.

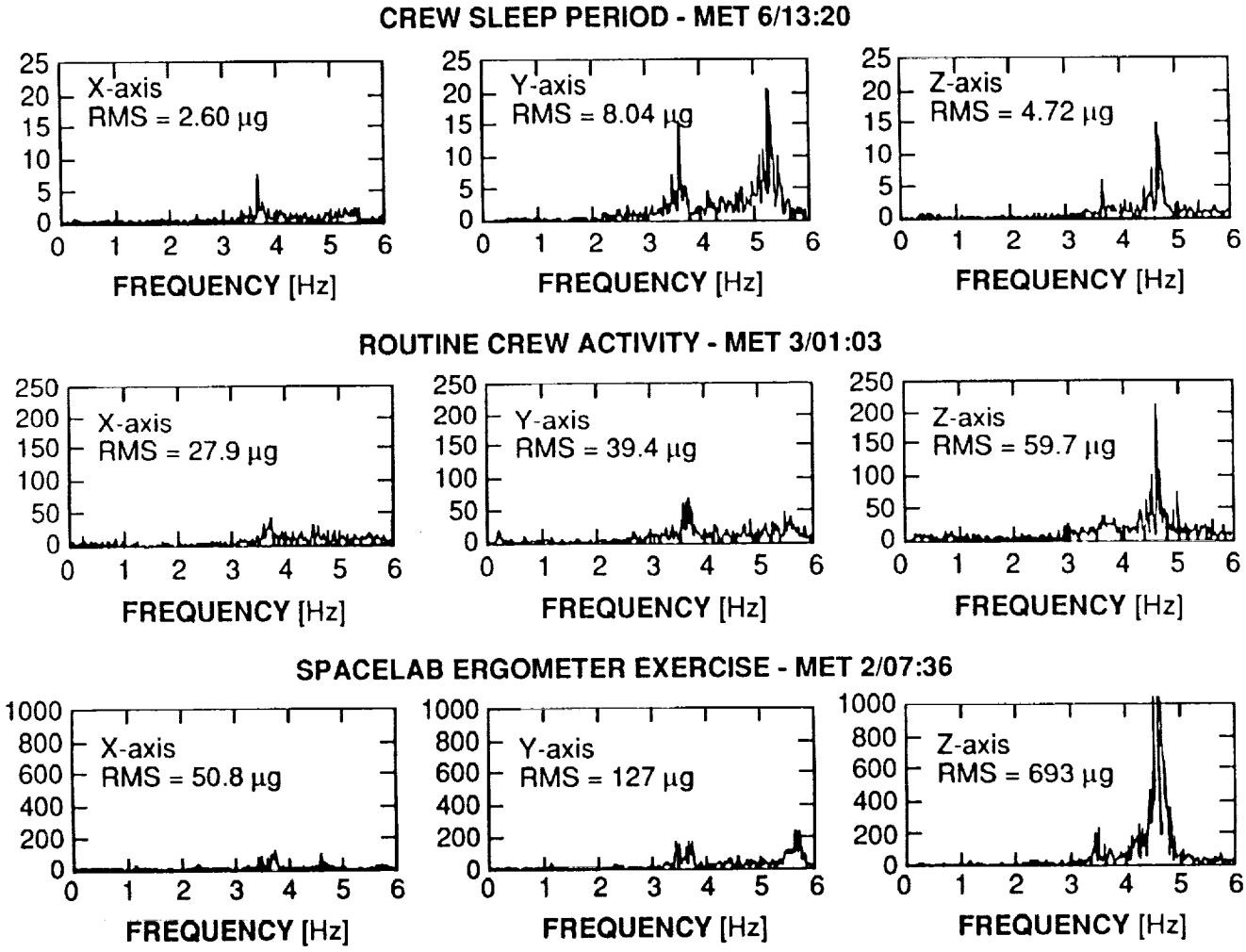

Figure 6 Power Spectral Density of the Acceleration environment on STS-40 - Spacelab module. Units of µg/√Hz.

STS-52

Time Referenced to MET 7/17:31

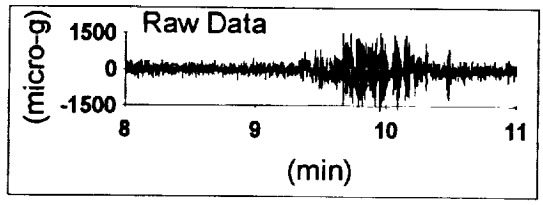

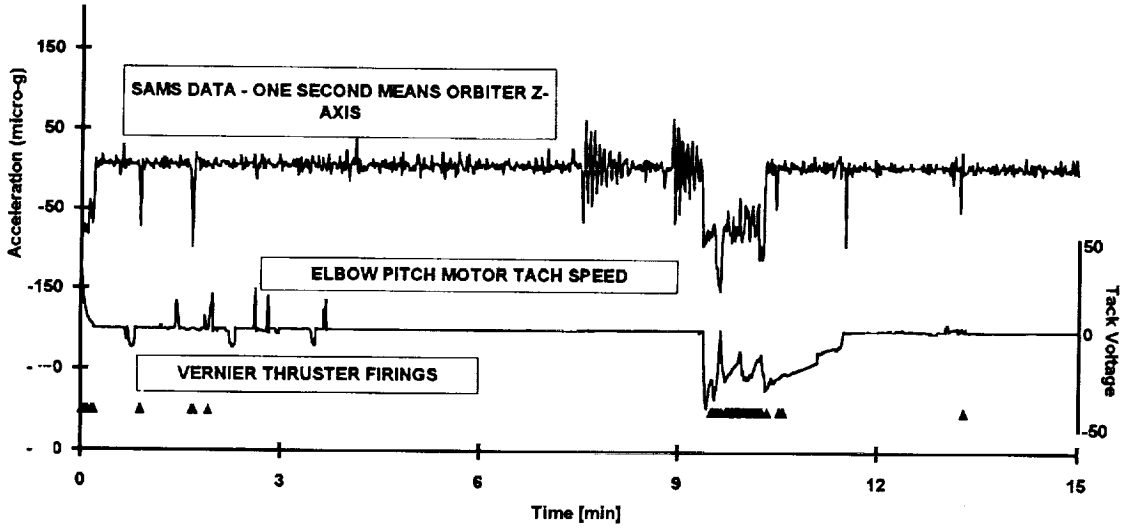

Figure 7 Analysis of Acceleration Disturbances from the Remote Manipulator arm.

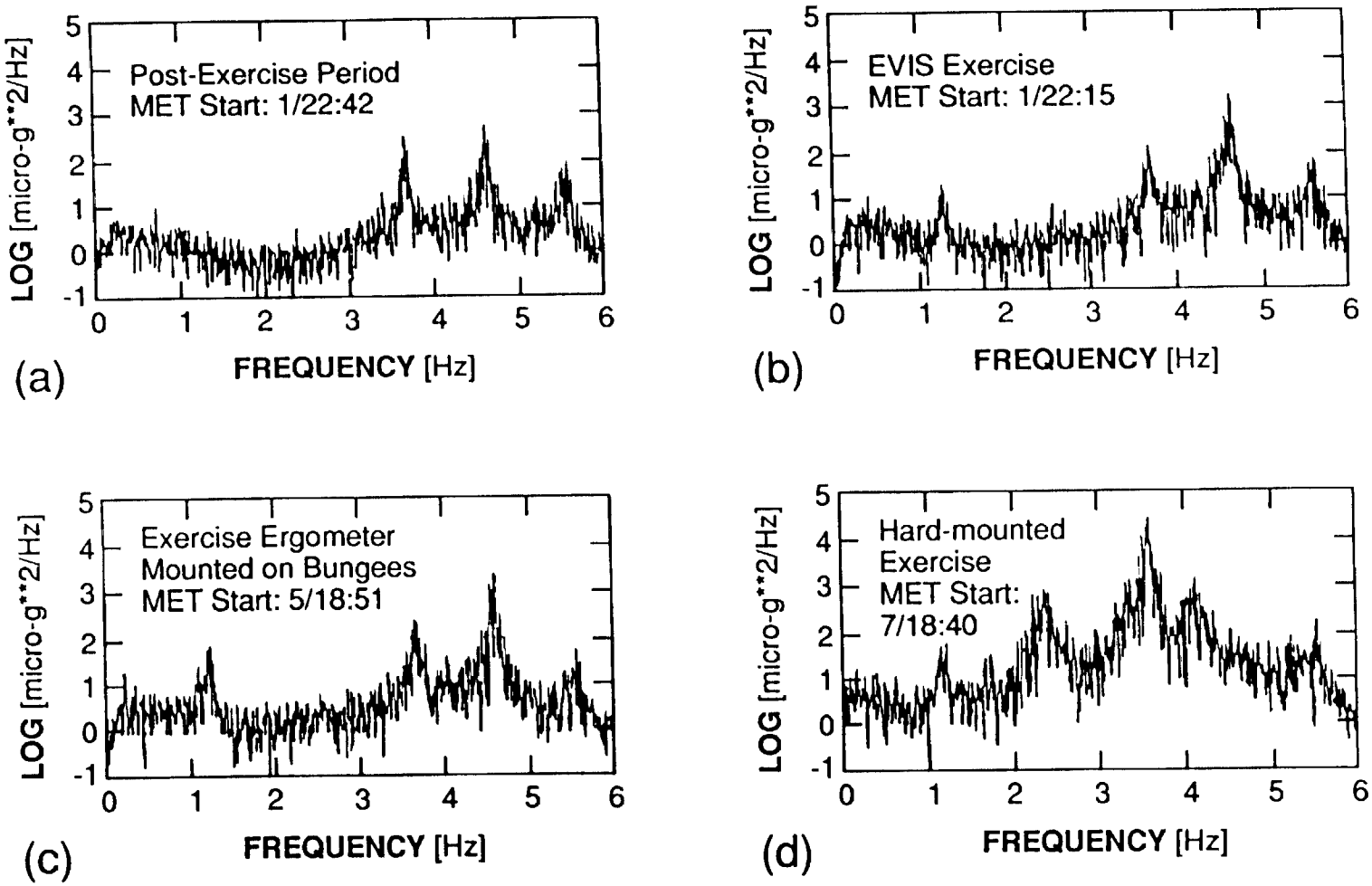

Figure 8 Power spectral density analysis of crew exercise, STS-50.

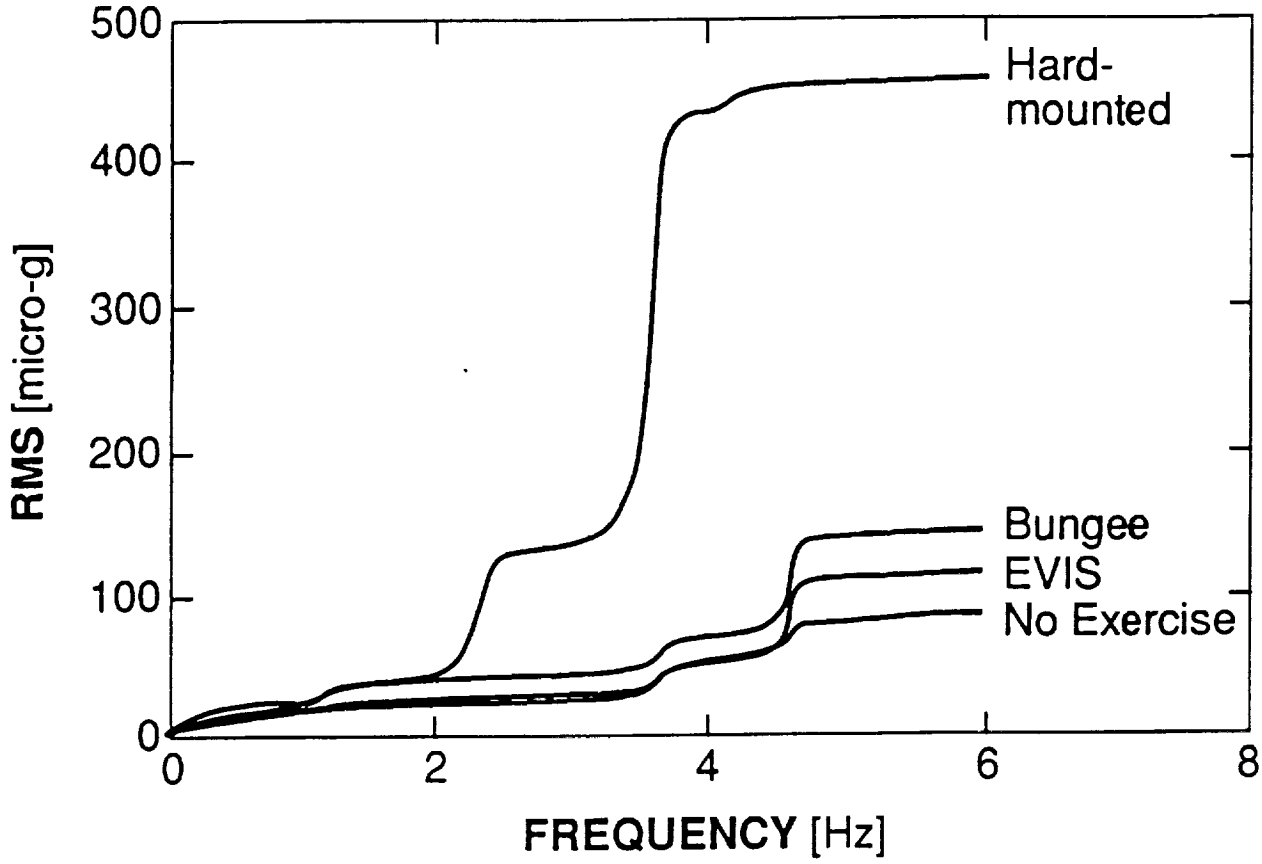

Figure 9 Cumulative RMS analysis of crew exercise, STS-50.

Discussion

Question: *This question is directed towards the previous two speakers. Having seen the data presented here by Charles Baugher, do they feel they are in any position to comment on if their particular experiments would be sensitive to either a) the described crew environment or b) to the disturbances in the upper two frequency bands that were described; 1 to 10 and 10 to 100 Hz ?*

Answer: In fact in the Lambda Point Experiment, we were very sensitive to the heating effects from vibration and were particularly concerned with the 51 Hz second harmonic from the TDRSS antenna because we have structural resonances quite close to that frequency. And as it turned out, because of the problems with the thermometry, we saw very little direct impact of the acceleration environment. On the next flight we expect to have that problem solved so we would be back in the situation where it would be significant again.

With regard to the MEPHISTO Experiment, acceleration effects on the experiment were clearly seen and the investigators are in the process of really vigorously looking at accelerometer data and correlating it with the Seebeck signals. As a matter of fact, Charles Baugher and Jean-Jacques Favier will be doing that for the next couple of months. As Favier showed in his presentation, there was definite correlation between acceleration and the experiment response.